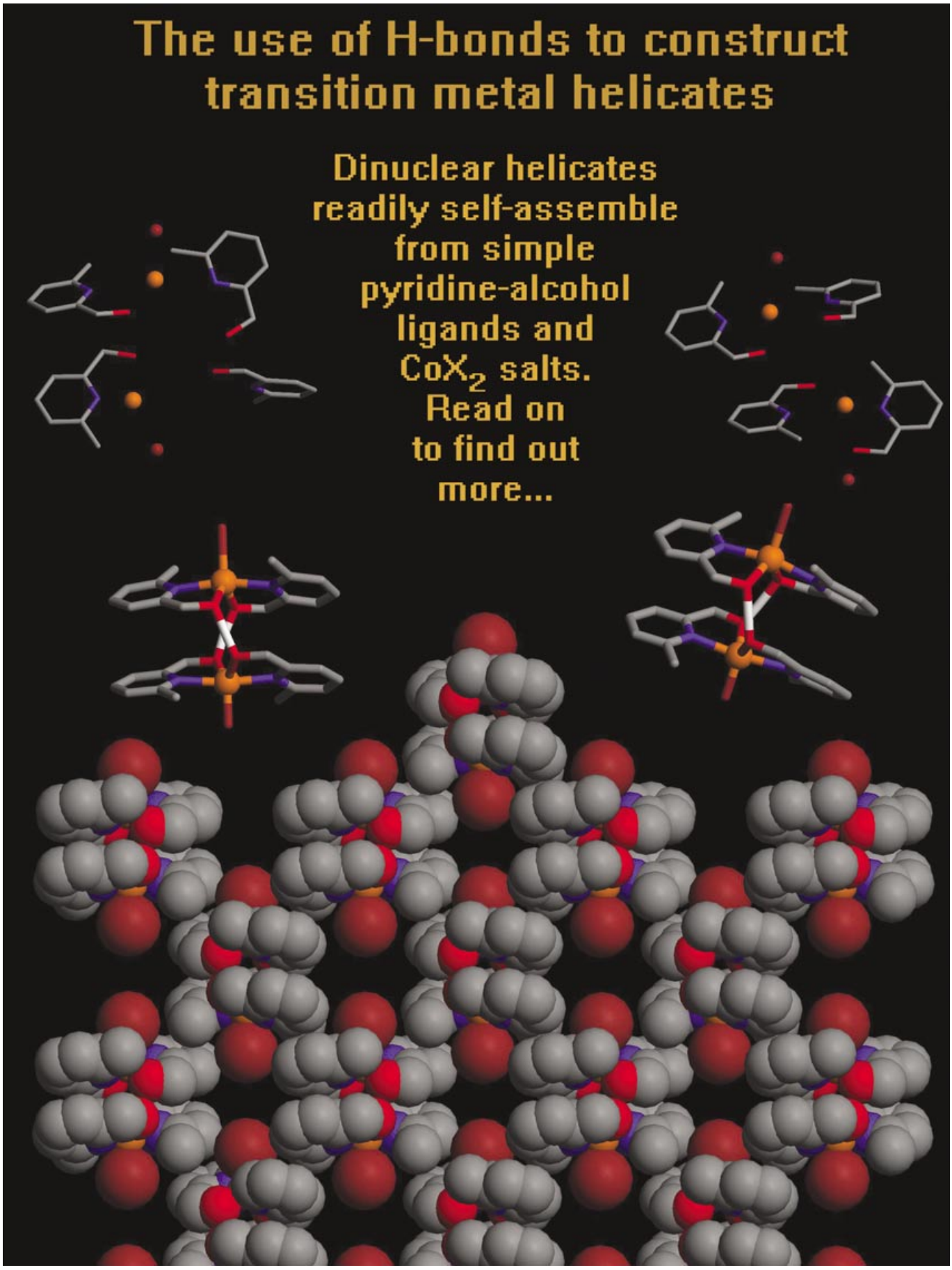

 DOI: 10.1002/chem.200400485

CHEMISTRY
A EUROPEAN JOURNAL

The Versatile, Efficient, and Stereoselective Self-Assembly of Transition-Metal Helicates by Using Hydrogen-Bonds

Shane G. Telfer*[a, c] and Reiko Kuroda*[a, b]

Abstract: A diverse range of dinuclear double-stranded helicates in which the ligand strand is built up by using hydrogen-bonding has been synthesized. The helicates, formulated as $[Co_2(L)_2(L\text{-}H)_2X_2]$, readily self-assemble from a mixture of a suitable pyridine–alcohol compound (L; for example, 6-methylpyridine-2-methanol, **1**), and a CoX_2 salt in the presence of base. Nine such helicates have been characterized by X-ray crystallography. For helicates derived from the same pyridine–alcohol precursor, a remarkable regularity was found for both the molecular structure and the crystal packing arrangements, regardless of the nature of the ancillary ligand (X). A notable exception was observed in the solid-state structure of $[Co_2(\mathbf{1})_2(\mathbf{1}\text{-}H)_2(NCS)_2]$ for which intermolecular nonbonded contacts between the sulfur atoms (S···S = 3.21 Å) lead to the formation of 1D chains. Helicates derived from (*R*)-6-methylpyridine-2-methanol (**2**) are soluble in solvents such as CH_3CN and CH_2Cl_2, and their self-assembly could be monitored in solution by ^1H NMR, UV/Vis, and CD titrations. No intermediate complexes were observed to form in a significant concentration at any point throughout these titrations. The global thermodynamic stability constant of $[Co_2(\mathbf{2})_2(\mathbf{2}\text{-}H)_2(NO_3)_2]$ was calculated from spectrophotometric data to be $\log\beta = 8.9(8)$. The stereoisomerism of these helicates was studied in some detail and the self-assembly process was found to be highly stereoselective. The chirality of the ligand precursors can control the absolute configuration of the metal centers and thus the overall helicity of the dinuclear assemblies. Furthermore, the enantiomers of *rac*-6-methylpyridine-2-methanol (**3**) undergo a self-recognition process to form exclusively homochiral helicates in which the four pyridine–alcohol units possess the same chirality.

Keywords: chirality · cobalt · helical structures · N,O ligands · self-assembly · supramolecular chemistry

Introduction

Transition-metal helicates have served as a pillar for the development of metallo-supramolecular chemistry over the past decade.[1,2] Helicates have formed the basis for numerous investigations that have contributed significantly to our understanding of metal-based self-assembly processes,[3] and to the stereoselective synthesis of metallo-supramolecular architectures.[4,5] The conventional synthetic route to helicates involves the mixing of a preformed ligand strand with an appropriate metal ion. In such systems, the ligand strand is almost always a covalent organic compound that has been synthesized by conventional methods. In a few cases, metal ions have been used to build up the ligand strand.[6]

We have recently presented a novel synthesis of transition-metal helicates that employs hydrogen bonding between the oxygen atoms of pyridyl-alcohol compounds (e.g., **1** to build up the ligand strands (Scheme 1).[7] These heli-

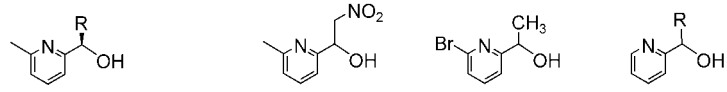

1 R = H
2 R = CH_3, *R* enantiomer
3 R = CH_3, *racemic* mixture

4

5

6 R = H
7 R = CH_3

[a] S. G. Telfer, R. Kuroda
JST ERATO Kuroda Chiromorphology Project, Park Bldg., 4–7–6 Komaba, Meguro-ku, Tokyo, 153-0041 (Japan)
Fax: (+81) 3-5465-0104
E-mail: shane.telfer@chiromor2.erato.rcast.u-tokyo.ac.jp
ckuroda@mail.ecc.u-tokyo.ac.jp

[b] R. Kuroda
Graduate School of Arts and Sciences, University of Tokyo, Komaba, Meguro-ku, Tokyo, 153–8902 (Japan)
Fax: (+81) 3-5452-0599

[c] S. G. Telfer
Current address:
Department of Chemistry, University of Montreal
CP 6128 succ. Centre-Ville, Montreal, QC, H3C 3J7 (Canada)

Supporting information for this article is available on the WWW under http://www.chemeurj.org/ or from the author.

DOI: 10.1002/chem.200400485

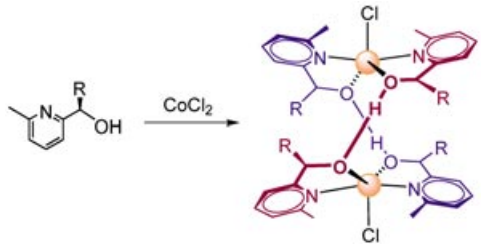

Scheme 1. The self-assembly of helicates using hydrogen bonding to build up the ligand strands.

cates self-assemble from eight simple components—four ions and four small molecules—and are stabilized by a variety of supramolecular interactions: coordination bonds, hydrogen bonds, and π–π interactions. This work compliments other recent advances in the fields of catalysis,[8] crystal engineering,[9] and other supramolecular assemblies,[10] which benefit from a fruitful combination of coordination and hydrogen bonding.

This approach has several notable advantages over the conventional synthesis of transition-metal helicates. The self-assembly step is a very rapid and straightforward "one-pot" procedure that simply involves combining suitable pyridine–alcohol precursors with cobalt(II) salts. A wide variety of such precursors is readily available, either commercially or by simple synthetic methods. This latter point means that the influence of the structure of the ligand strand precursor on the self-assembly process may be systematically investigated. Further diversity may potentially be introduced into the dinuclear assemblies by changing the metal ion and/or the ancillary ligand.

Herein, we present the full details of our recent investigations into the use of hydrogen-bonding as a construction element for the ligand strands of transition-metal helicates. We have focused on the reaction of precursors **1**–**3** with a wide range of cobalt(II) salts (Scheme 1). We have found that the self-assembly process is both versatile and high-yielding, and complete diastereoselectivity may be observed in both solution and the solid state.

Results

Synthesis of helicates derived from 1–3: The original synthetic route that we reported for the hydrogen-bonded helicates derived from **1** and **2** involved the reaction of these precursors with $CoCl_2 \cdot 6H_2O$ and $Co(OAc)_2 \cdot 4H_2O$ in a MeOH/dioxane solvent mixture.[7] Whilst this method leads to a good yield of $[Co_2(\mathbf{1})_2(\mathbf{1}\text{-}H)_2Cl_2]$, the yield of other $[Co_2(\mathbf{1})_2(\mathbf{1}\text{-}H)_2X_2]$ helicates (e.g., X = Br, I, NO_3) was much lower (< 15%). The reason for these low yields is not clear, though we suspect that the acetate ions may promote the formation of cluster complexes.

A number of variations were introduced into the synthetic scheme in an effort to improve these yields and to formulate a more general synthetic route. The replacement of the acetate ions by the alternative bases NaOH and NEt_3 led to mixtures of crystalline products that were identified by X-ray crystallography as $[Co_2(\mathbf{1})_2(\mathbf{1}\text{-}H)_2X_2]$ and $[Co_4(\mathbf{1}\text{-}H)_4X_2(MeOH)_2]$. The formation of the tetranuclear cluster complexes, which will be detailed in a separate publication, can be ascribed to the stronger basicity of both NaOH and NEt_3 as compared to acetate. To circumvent the formation of these clusters, we supposed that compound **1** may be able to act as the requisite base. Indeed, the reaction of a variety of CoX_2 salts with four equivalents of **1** in CH_3CN was found to lead to the rapid crystallization of analytically pure $[Co_2(\mathbf{1})_2(\mathbf{1}\text{-}H)_2X_2]$ helicates. The insolubility of these helicates greatly facilitates their isolation—they are easily separated from $[\mathbf{1}\text{-}H]^+$ (which can be recovered if necessary) and any side products by simple filtration and washing. This synthetic route proved to be both general and straightforward. The yield of the helicates was high, ranging from 73% for $X = NO_3$ to 90% for X = Br. X-ray quality crystals of the $[Co_2(\mathbf{1})_2(\mathbf{1}\text{-}H)_2X_2]$ helicates were prepared by performing the same reaction in MeOH, although the overall yields were somewhat depressed using this solvent.

Using the general method of Ikariya et al.,[11] we were able to prepare the chiral compound (*R*)-**2** (henceforth referred to as **2**) in 93% *ee* by the asymmetric hydrogenation of 2-acetyl-6-methylpyridine. The reaction of **2** with CoX_2 salts in the presence of base also leads to the formation of dinuclear double-stranded helicates that can be formulated as $[Co_2(\mathbf{2})_2(\mathbf{2}\text{-}H)_2X_2]$. We found that compound **2** is far less disposed than **1** to the formation of high nuclearity cluster complexes in the presence of strong bases such as NEt_3. The highest yielding synthetic procedure, however, involved the combination of one equivalent each of CoX_2 and $Co(OAc)_2$ with two equivalents of **2**. Upon concentration of the solution, crimson-colored (X = Cl, Br) or rose-colored ($X = NO_3$) crystals of $[Co_2(\mathbf{2})_2(\mathbf{2}\text{-}H)_2X_2]$ deposited in good yield. Similar observations were made when compound **3** (the racemic analogue of **2**) was used to prepare the helicates.

All of the new compounds described herein are air-stable in the solid state and may be stored over long periods without noticeable decomposition. The solubilities of the helicates derived from **1**–**3** in non-aqueous polar solvents are noticeably different, decreasing in the order **2** (generally highly soluble), **3** (somewhat soluble), **1** (virtually insoluble). Where soluble, the helicates were found to fairly stable (at high concentrations, vide infra) in solvents such as CH_3OH, CH_3CN, CH_3NO_2, and CH_2Cl_2, however they decomposed in DMSO, probably due to rupture of the hydrogen bonds.

Solid-state structures of helicates derived from 1: The solid-state structures of a range of $[Co_2(\mathbf{1})_2(\mathbf{1}\text{-}H)_2X_2]$ helicates (X = Cl, Br, I, NO_3, SCN) has been determined by X-ray crystallography (Table 1). The structures of the first four of these helicates are remarkably similar, and will be discussed first. The packing arrangement of the SCN-containing helicate is particularly interesting and will be discussed subsequently.

The molecular structure of the hydrogen-bonded helicates is exemplified by the structure of $[Co_2(\mathbf{1})_2(\mathbf{1}\text{-}H)_2Br_2]$

Table 1. Crystallographic data for the $[Co_2(\mathbf{1})_2(\mathbf{1}\text{-H})_2X_2]$ helicates.

X	Cl	Br	I	NO_3	SCN
crystal system	orthorhombic	orthorhombic	orthorhombic	orthorhombic	orthorhombic
space group	*Pbcn*	*Pbcn*	*Pbcn*	*Pbcn*	$Pca2_1$
a [Å]	14.4508(7)	14.498(1)	14.6153(7)	14.681(1)	16.850(1)
b [Å]	15.1817(8)	15.243(1)	15.2092(7)	15.643(1)	13.664(1)
c [Å]	13.5843(7)	13.483(1)	13.7119(6)	13.506(1)	14.021(1)
V [Å^3]	2980.2(3)	2979.9(3)	3048.0(2)	3101.7(4)	3228.2(4)
R	0.0495	0.0336	0.0242	0.0370	0.0298
wR_2 (all data)	0.1538	0.0861	0.0586	0.0880	0.0760
Selected distances [Å]					
Co···Co	4.38	4.37	4.34	4.43	4.36
O^{py}–O^{py}[a]	2.42	2.43	2.41	2.42	2.42
Co–N	2.13, 2.15	2.13, 2.15	2.13, 2.16	2.13, 2.16	
Co–O^{py}	1.99, 2.00	1.99, 2.00	1.99, 2.00	1.99, 2.00	1.99
Co–X	2.31, 2.34	2.47	2.67, 2.70	2.20, 2.21	1.98
Co–X···X–Co[b]	10.80	10.87	10.87	11.21	12.52
Selected angles [°]					
N-Co-N	167.9, 171.7	167.2, 172.8	166.9, 172.9	167.6, 174.1	174.0, 174.6
O^{py}-Co-O^{py}	113.8, 117.9	114.0, 118.7	114.6, 118.5	111.4, 116.9	115.7, 116.2
O^{py}-H-O^{py}	173.3	179.4	175.5	170.0	177.2, 177.4

[a] O^{py} refers to the oxygen atoms of **1**. [b] The Co–X···X–Co distance refers to intermolecular separation of the Co centers of the rows of helicates aligned along the crystallographic *b* axis.

(Figure 1). The ligand strands are composed of a pair of hydrogen-bonded molecules of **1**, and this strand coordinates to two cobalt(II) atoms in a bis(bidentate) fashion through its pyridyl and alcohol donor groups. Two such ligand strands wrap around an axis defined by the two cobalt(II) centers. When the ancillary ligand coordinates in a monodentate fashion (X = Cl, Br, I), the geometry of these metal centers is roughly trigonal bypyramidal with the N-Co-N vector describing the psuedo-C_3 axis. The nitrate ion was found to adopt a bidentate coordination mode, and the geometry of the metal centers in $[Co_2(\mathbf{1})_2(\mathbf{1}\text{-H})_2(NO_3)_2]$ is best described as distorted octahedral.

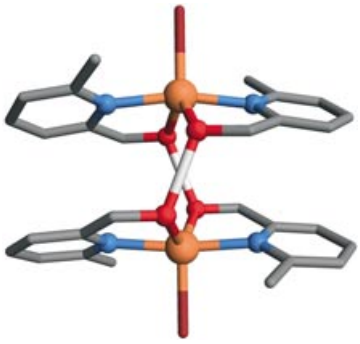

Figure 1. X-ray crystal structure of the $[Co_2(\mathbf{1})_2(\mathbf{1}\text{-H})_2Br_2]$ helicate. Hydrogen atoms omitted for clarity. Co: orange; N: blue; O: red; Br: dark red.

The structural similarity of the series of helicates derived from compound **1** (X = Cl, Br, I and NO_3) is highlighted by Figure 2 which shows an overlay of the solid-state structures of these four complexes. Many geometrical parameters are observed to be fairly constant within this series, for example, the metal–ligand bond lengths, the Co···Co separation, and the distance between the hydrogen-bonding oxygen atoms (Table 1). As expected, the bidentate coordination mode of the NO_3^- ligand leads to a slight compression of the O^{py}-Co-O^{py} angles (O^{py} = coordinating oxygen atom of the pyridine–alcohol ligand), and the Co···Co distance is slightly elongated as a consequence.

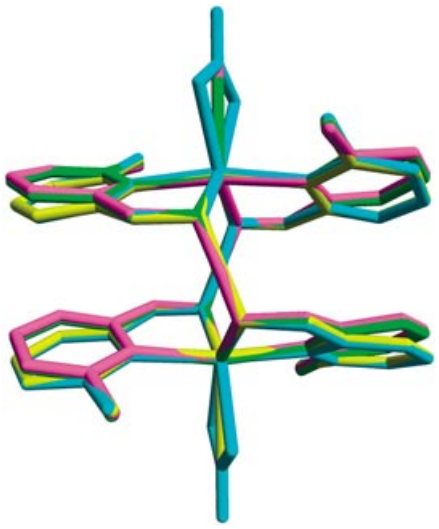

Figure 2. Overlay of the skeletons of the molecular structures of four $[Co_2(\mathbf{1})_2(\mathbf{1}\text{-H})_2X_2]$ helicates. X = Cl: green; X = Br: yellow; X = I: pink; X = NO_3: blue.

These four $[Co_2(\mathbf{1})_2(\mathbf{1}\text{-H})_2X_2]$ helicates (X = Cl, Br, I, NO_3) are virtually isostructural: they crystallize in the same space group (*Pbcn*) and display very similar unit cell dimensions and packing arrangements. A packing diagram of $[Co_2(\mathbf{1})_2(\mathbf{1}\text{-H})_2XBr_2]$ is shown as an example in Figure 3. It can be seen that the helicates align in and 'end-to-end' fashion to form rows along the crystallographic *b* axis. These

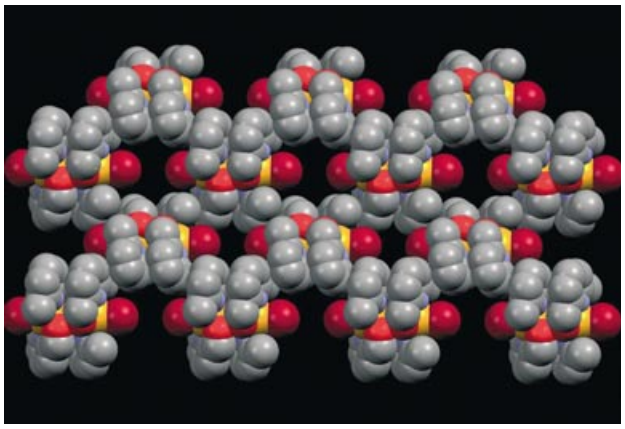

Figure 3. The $[Co_2(\mathbf{1})_2(\mathbf{1}\text{-H})_2Br_2]$ helicates forms homochiral rows of helicates along the crystallographic *b* axis. Hydrogen atoms omitted for clarity. Co: orange; N: blue; O: red; Br: dark red.

rows are homochiral, that is each constituent helicate has the same (*P* or *M*) helicity. Alternating rows of *P* and *M* helicates build up the layer (the crystal is racemic overall). The *intermolecular* Co···Co distance between the helicates aligned along the *b* axis is 10.87 Å, and a similar distance is observed for the other helicates in this series (Table 1). Closer contact is prevented by intermolecular interactions of the pyridyl groups of the helicates of neighboring rows. Within each row, there is a significant gap between the ancillary bromo ligands of the individual helicates and a distinct cavity is formed in the vicinity of these ligands. The presence of this cavity offers a plausible explanation for the conservation of the packing arrangement in this series of helicates: ancillary ligands of different sizes may occupy sites near this cavity without disturbing the overall packing arrangement.[12]

The X-ray crystal structure of the $[Co_2(\mathbf{1})_2(\mathbf{1}\text{-H})_2(NCS)_2]$ helicate reveals that its molecular structure is nearly identical to the other helicates formed from precursor **1** (Table 1). As expected, the SCN auxiliary ligand coordinates through its nitrogen atom. Although this helicate crystallizes in a different space group, its overall packing arrangement is roughly similar to the other members of this series of helicates. In this case, however, the S atoms of the SCN ligands of neighboring helicates are separated by a distance of 3.21 Å. This is considerably shorter than sum of the van der Waals radii of these atoms (3.60 Å),[13] and is indicative of attractive contacts between these S atoms. These contacts link the helicates into a 1D chain along the crystallographic *a* axis (Figure 4). These chains are homochiral, that is, contacts exist only between helicates of the same left- or right-handed chirality. Overall the crystal is racemic: chains of alternating chirality are arranged in zigzag rows in the crystallographic *ab* plane.

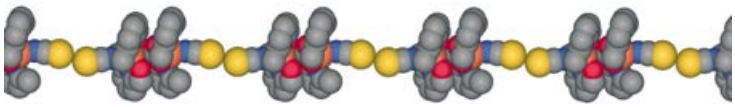

Figure 4. Formation of a 1D chain along the *a* axis in the solid state structure of $[Co_2(\mathbf{1})_2(\mathbf{1}\text{-H})_2(NCS)_2]$. Co: orange; N: blue; O: red; S: yellow.

Solid-state structures of helicates derived from 2: The solid state structures of a series of $[Co_2(\mathbf{2})_2(\mathbf{2}\text{-H})_2X_2]$ helicates (X = Cl, Br, NO_3) were determined by X-ray crystallography and selected crystallographic data are presented in Table 2.

Table 2. Crystallographic data for $[Co_2(\mathbf{2})_2(\mathbf{2}\text{-H})_2X_2]$ helicates.

Ancillary ligand (X)	Cl	Br	NO_3
crystal system	orthorhombic	monoclinic	monoclinic
space group	$P2_12_12$	$P2_1$	$P2_1$
a [Å]	11.4404(2)	12.2145(6)	12.263(2)
b [Å]	17.704(2)	11.2358(5)	11.587(2)
c [Å]	9.4371(1)	12.8948(6)	12.980(2)
β [°]	N/A	98.258(1)	98.723(3)
V [Å^3]	1911.4(3)	1751.3(1)	1822.9(5)
R	0.0654	0.0260	0.0455
wR_2 (all data)	0.1415	0.0537	0.0939
Selected distances [Å]			
Co···Co	4.325	4.384	4.507
O–O	2.424, 2.441	2.427, 2.422	2.428
Co–N	2.125, 2.146	2.138–2.147	2.137–2.152
Co–O	1.964, 2.000	1.967–1.984	1.973–2.216
Co–X	2.344	2.473, 2.480	2.216–2.253
Selected angles [°]			
N-Co-N	170.1	167.9, 169.79	169.3, 170.6
O-Co-O	118.2	116.48, 116.56	110.6, 112.2
O-H-O	179.9	172.97, 177.01	170.0

The molecular structure of $[Co_2(\mathbf{2})_2(\mathbf{2}\text{-H})_2(NO_3)_2]$ is shown as a representative example in Figure 5. The molecular structures of the chloride- and bromide-containing helicates were found to be very similar. Similarities may also be noted between the helicates derived from **2** and those derived from **1**. This is highlighted by Figure S1 in the Sup-

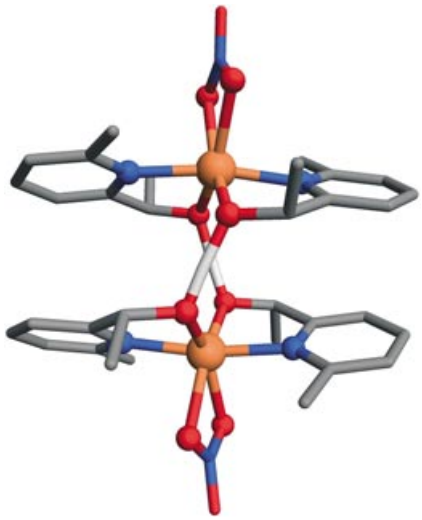

Figure 5. X-ray crystal structure of $[Co_2(\mathbf{2})_2(\mathbf{2}\text{-H})_2(NO_3)_2]$. Co: orange; N: blue; O: red.

porting Information, which shows an overlay of the skeletons of $[Co_2(\mathbf{1})_2(\mathbf{1}\text{-H})_2Br_2]$ and $[Co_2(\mathbf{2})_2(\mathbf{2}\text{-H})_2Br_2]$.

Only one diastereomer is observed in the solid state structures of the three helicates derived from compound **2**. In all cases, the chirality of the ligand precursor **2** is efficiently transferred to the helicate structure: the cobalt(II) centers adopt the *Λ* absolute configuration and the ligand strands wrap around the Co···Co axis in a right-handed (*P*) fashion.

Solution behavior of $[Co_2(2)_2(2\text{-H})_2X_2]$ helicates

Spectroscopic characterization of $[Co_2(\mathbf{2})_2(\mathbf{2}\text{-H})_2X_2]$ (X = Cl, Br, NO_3) helicates in solution: The ^{1}H NMR spectra of the three $[Co_2(\mathbf{2})_2(\mathbf{2}\text{-H})_2X_2]$ helicates (X = Cl, Br, NO_3) dissolved in CD_3CN all display a set of six peaks paramagnetically shifted over a range of around 60 ppm. This suggests that the structure observed by X-ray crystallography is maintained in solution and that the complexes have average D_2 symmetry. Furthermore, the observation of just one set of peaks in all cases demonstrates that the three $[Co_2(\mathbf{2})_2(\mathbf{2}\text{-H})_2X_2]$ helicates are formed in solution with high (>95%) diastereoselectivity.

CD spectroscopy also reflects both the similarity of the solid state and solution structures and the high diastereoselectivity of helicate formation. The CD spectra of $[Co_2(\mathbf{2})_2(\mathbf{2}\text{-H})_2Cl_2]$ recorded in CH_3CN solution and as a KBr disc are presented in Figure 6. The spectra show a close resemblance, displaying three Cotton effects in the range 300–900 nm which can be assigned to d–d transitions of the cobalt(II) centers.

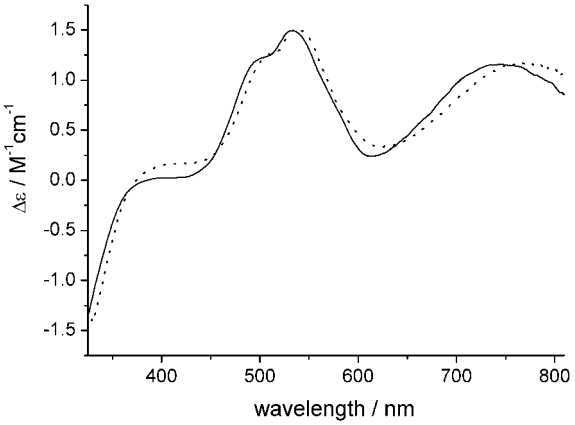

Figure 6. CD spectra of $[Co_2(\mathbf{2})(\mathbf{2}\text{-H})_2Cl_2]$ in solution (5.5×10^{-3} M, CH_3CN, full line) and in the solid state (KBr disc, dotted line). The solid-state spectrum has been normalized to the solution spectrum at 532 nm.

The electrospray mass spectra of the three helicates were measured in CH_3CN. Although the neutral helicates cannot be observed directly, very intense peaks corresponding to the fragmentation products $[Co_2(\mathbf{2})(\mathbf{2}\text{-H})_2X]^+$ were observed.

Monitoring the formation of $[Co_2(\mathbf{2})_2(\mathbf{2}\text{-H})_2X_2]$ in solution: A series of titration experiments was performed in order to investigate the self assembly reaction leading to the $[Co_2(\mathbf{2})_2(\mathbf{2}\text{-H})_2X_2]$ helicates in solution. The reaction could be monitored by UV/Vis, CD, and ^{1}H NMR spectroscopies. Spectral changes were monitored as CoX_2 salts were added to a solution of **2** using either NEt_3 (method 1) or $Co(OAc)_2$ (method 2) as the requisite base. The two methods produced similar results.

$$4\,\mathbf{2} + 2\,NEt_3 + 2\,CoCl_2 \rightarrow [Co_2(\mathbf{2})_2(\mathbf{2}{-}H)_2Cl_2] + 2\,HNEt_3Cl \quad \text{(method 1)}$$

$$4\,\mathbf{2} + CoCl_2 + Co(OAc)_2 \rightarrow [Co_2(\mathbf{2})_2(\mathbf{2}{-}H)_2Cl_2] + 2\,HOAc \quad \text{(method 2)}$$

The results of the ^{1}H NMR titration using Method 1 are presented in Figure 7. As the titration progressed, the diamagnetic peaks of free (*R*)-**2** were steadily replaced by a single set of paramagnetically shifted peaks. These paramagnetically shifted peaks can be assigned to the $[Co_2(\mathbf{2})_2(\mathbf{2}\text{-}\mathbf{H})_2Cl_2]$ helicate by comparison with the spectrum of an authentic sample, and represent the only detectable product at all stages of the titration. A small amount of free **2** remains observable at a Co/**2** ratio of 1/2, however the addition of further cobalt(II) led to severe broadening of the signals.

The formation of $[Co_2(\mathbf{2})_2(\mathbf{2}\text{-H})_2Cl_2]$ could be monitored by CD spectroscopy in the visible wavelength range (400–800 nm) using titration method 1 (see Figure S3 in the Supporting Information). A solution with a fairly high concentration of **2** (ca. 0.014 M) was employed due to the rather weak intensity of the CD spectrum in this region. A steady increase in signal intensity was observed up to a Co/**2** ratio of 1/2, with an isosbestic point appearing at 410 nm. The similarity in the shape of all these spectra, and the presence of the isosbestic point, strongly suggest that only one chiral product is formed when $CoCl_2$, **2**, and NEt_3 are combined in CH_3CN. The identity of this product—$[Co_2(\mathbf{2})_2(\mathbf{2}\text{-H})_2Cl_2]$—was confirmed by measuring the CD spectrum of an independent sample.

Although only minor changes were observed in the high energy (200–350 nm) region of the UV/Vis spectrum, the formation of $[Co_2(\mathbf{2})_2(\mathbf{2}\text{-H})_2(NO_3)_2]$ could be conveniently monitored in the visible (380–900 nm) region. An absorbance band around 500 nm, along with weaker bands at lower energies, were observed to steadily rise in intensity as the titration progressed (see Figure S2 in the Supporting Information).

A series of careful spectrophotometric titrations were carried out in order to determine the global stability constant of $[Co_2(\mathbf{2})_2(\mathbf{2}\text{-H})_2(NO_3)_2]$. The data were analysed with the Specfit program,[14] and were successfully fitted using a chemical model with $[Co_2(\mathbf{2})_2(\mathbf{2}\text{-H})_2(NO_3)_2]$ and "free" cobalt(II) as the absorbing species.[15] The inclusion of other absorbing species such as $[Co(\mathbf{2})_2]$ dramatically worsened the fit to the data. The global stability constant calculated for $[Co_2(\mathbf{2})_2(\mathbf{2}\text{-H})_2(NO_3)_2]$ was $\log\beta_{24} = 8.9(8)$ (Eq. (1)). The absorption spectra predicted by the fitting process for

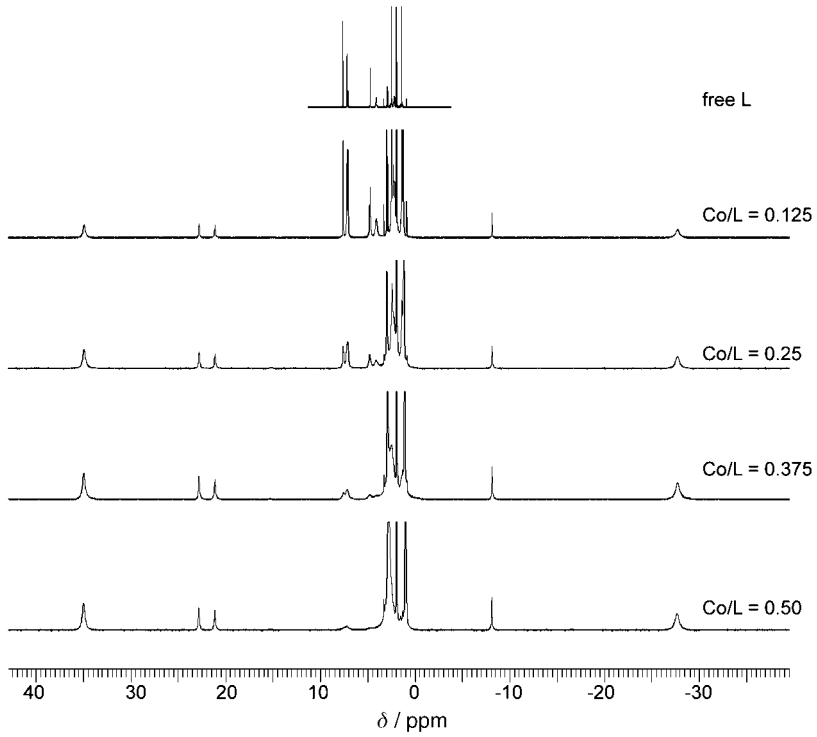

Figure 7. ^{1}H NMR spectra monitoring the titration of *R*-**2** with $CoCl_2$ and NEt_3 in CD_3CN. The intense peaks in the region 0–4 ppm are due to residual solvent and $HNEt_3^+$ and obscure one of the signals of $[Co_2(\mathbf{2})_2(\mathbf{2}\text{-H})_2Cl_2]$. [**2**] = ca. 0.1 M.

$[Co_2(\mathbf{2})_2(\mathbf{2}\text{-H})_2(NO_3)_2]$ and free cobalt(II) were in very good agreement with independently measured spectra.

$$2\,Co^{II} + 4\,\mathbf{2} \overset{K_{24}}{\rightleftharpoons} [Co_2(\mathbf{2})_2(\mathbf{2}\text{-H})_2] + 2\,H^+ \qquad (1)$$

Speciation curves showing the distribution of free **2** and $[Co_2(\mathbf{2})_2(\mathbf{2}\text{-H})_2(NO_3)_2]$ were simulated using the calculated stability constant (Figure 8). For an initial concentration of **2** of 0.12 M, the addition of $Co(NO_3)$ initially leads to a near-linear rise in the concentration of $[Co_2(\mathbf{2})_2(\mathbf{2}\text{-H})_2(NO_3)_2]$. The formation of this complex tails off at higher Co/**2** ratios. Despite its high concentration, only around 80% of **2** is coordinated at a Co/**2** ratio of 1/2. This is in full accord with the ^{1}H NMR titrations presented above where signals corresponding to free **2** were still observable at a Co/**2** ratio of 1/2 (Figure 7).

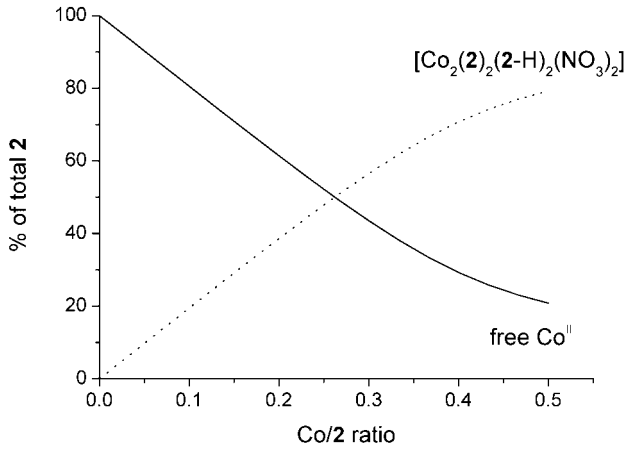

Figure 8. Simulated speciation curve showing distribution of free **2** (full line) and $[Co_2(\mathbf{2})_2(\mathbf{2}\text{-H})_2Cl_2]$ (dotted line) during the titration of **2**/NEt_3 (2/1 ratio) with $Co(NO_3)\cdot 6H_2O$ in CH_3CN. Curves calculated using a $\log\beta_{24}$ value of 8.9, and with an initial concentration of **2** of 0.12 M.

Behavior of the $[Co_2(\mathbf{2})_2(\mathbf{2}\text{-H})_2X_2]$ helicates in dilute solution: The behavior of the $[Co_2(\mathbf{2})_2(\mathbf{2}\text{-H})_2Cl_2]$ helicate in dilute solution was probed by CD, UV/Vis, and ^{1}H NMR spectroscopies. CD spectra of this complex recorded in the concentration range 22.0–0.1 × 10^{-3} M are presented in Figure 9. The ordinate scale corresponds to $\Delta\varepsilon$ values based on the total concentration of **2**. A dramatic change was observed in the CD spectra as the solution was diluted: the positive Cotton effect centred around 270 nm inverted to give a negative Cotton effect. The changes to the UV spectrum in this concentration range were much more subtle with a slight (ca. 10%) rise in intensity noted for the peak at 263 nm.

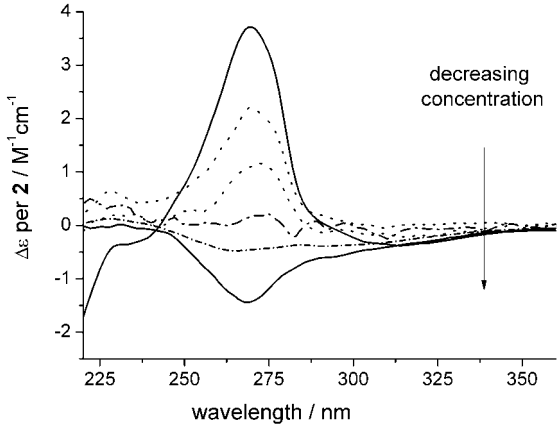

Figure 9. The inversion of the CD spectrum of $[Co_2(\mathbf{2})_2(\mathbf{2}\text{-H})_2Cl_2]$ as the concentration is lowered. Spectra measured in CH_3CN with effective concentrations of **2** of 22.0, 4.0, 2.0, 1.0, 0.5, 0.2, and 0.1 × 10^{-3} M.

By comparison with an independent sample, the CD spectrum recorded at the lowest concentration can be attributed

to free **2**. This is supported by corresponding ^{1}H NMR experiments where the paramagnetic peaks due to the $[Co_2(\mathbf{2})_2(\mathbf{2}\text{-H})_2Cl_2]$ helicate were gradually replaced by a set of diamagnetic peaks corresponding to free **2** as the sample was diluted (see Figure S4 in the Supporting Information).

Helicates derived from 3: Hydrogen-bonded helicates could also be prepared from the racemic pyridine-ethanol precursor **3**. Crimson-colored prismatic crystals of $[Co_2(\mathbf{3})_2(\mathbf{3}\text{-H})_2Cl_2]$ suitable for X-ray crystallography were obtained by recrystallisation from hot CH_3NO_2. The helicate was found to crystallize in the space group $P2_1/n$, and although the poor quality of the diffraction data preclude analysis of the fine details of the structure, the overall geometry and packing arrangement of the complex is clear. Selected crystallographic data and geometrical parameters are listed in Table 3, and by comparison with the geometrical parameters of the enantiopure $[Co_2(\mathbf{2})_2(\mathbf{2}\text{-H})_2X_2]$ helicates (Table 2), it can be seen that the molecular structures of the two types of helicates are very similar.

Table 3. Crystallographic data for the $[Co_2(\mathbf{3})_2(\mathbf{3}\text{-H})_2Cl_2]$ helicate.

crystal system	monoclinic
space group	$P2_1/n$
a [Å]	14.401(1)
b [Å]	16.311(1)
c [Å]	16.771(1)
β [°]	90.187(1)
V [Å^3]	3941.9(5)
R	0.1489
wR_2 (all data)	0.3478
Selected distances [Å]	
Co···Co	4.402
O–O	2.43
Co–N	2.13–2.14
Co–O	1.97–1.99
Co–Cl	2.32–2.33
Selected angles [°]	
N-Co-N	169.7–170.0
O-Co-O	114.9–116.5

The crystal structure is composed of an enantiomeric pair of helicates: Λ,Λ-$[Co_2((R)\text{-}\mathbf{3})_2((R)\text{-}\mathbf{3}\text{-H})_2Cl_2]$ and Δ,Δ-$[Co_2((S)\text{-}\mathbf{3})_2((S)\text{-}\mathbf{3}\text{-H})_2Cl_2]$. The ligand strands in these complexes describe right- and left-handed helices (i.e., *P* and *M* helices) respectively. Helicates of the same helicity pack in an end-to-end fashion to form homochiral columns along the crystallographic *a* axis. Columns of alternating chirality are held together by π–π interactions between the pyridyl groups (interplane distances = ca. 3.6 Å) of neighboring helicates to form sheets in the *ac* crystallographic plane (Figure 10). This packing arrangement is reminiscent of that observed for the racemic $[Co_2(\mathbf{1})_2(\mathbf{1}\text{-H})_2X_2]$ helicates.

^{1}H NMR spectroscopy shows that $[Co_2(\mathbf{3})(\mathbf{3}\text{-H})_2Cl_2]$ remains intact in solution at relatively high concentrations. A spectrum of dissolved crystals recorded in CD_2Cl_2 displays a set of five peaks paramagnetically shifted over a range of

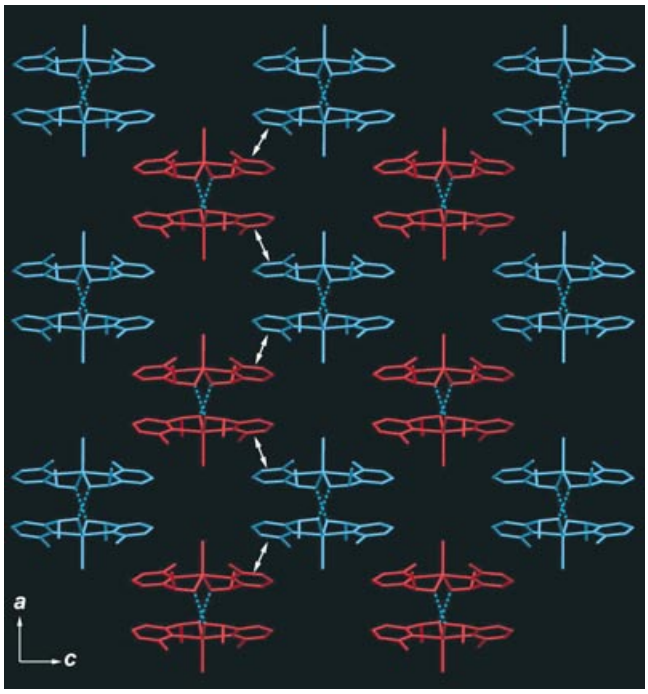

Figure 10. The packing arrangement of Λ,Λ-$[Co_2((R)\text{-}\mathbf{3})_2((R)\text{-}\mathbf{3}\text{-H})_2Cl_2]$ (blue) and Δ,Δ-$[Co_2((S)\text{-}\mathbf{3})_2((S)\text{-}\mathbf{3}\text{-H})_2Cl_2]$ (red) in the solid state. The double-headed white arrows indicate π-π interactions between the pyridyl groups of neighboring helicates, and the dotted blue lines represent hydrogen bonds. Solvent molecules (CH_3NO_2) which fill the voids between the helicates are omitted.

65 ppm. Six peaks are expected if the D_2 symmetry of the helicates structure is maintained in solution, however it appears that one of the peaks is obscured by the signal due to residual H_2O around 1.5 ppm. This spectrum is practically identical to the spectrum of $[Co_2(\mathbf{2})(\mathbf{2}\text{-H})_2Cl_2]$ recorded in CD_2Cl_2, with the same peaks observed at the same chemical shifts (±0.3 ppm). No signals corresponding to any other paramagnetic complexes were detected.

The attempted synthesis of helicates using precursor 5: The pyridyl-alcohol ligand precursor **5**, which has a bromo substituent in place of the usual methyl group, is easily prepared via reduction of commercially available 2-bromo-6-acetylpyridine with $NaBH_4$. Upon mixing **5** with 0.25 equivalents each of $CoCl_2$ and $Co(OAc)_2$, either a blue solution (CH_3CN) or a practically colorless solution (CH_3OH) was observed. Blue oils formed when these solutions were concentrated under reduced pressure. Crystalline products could not be obtained from solutions of these oils in spite of attempts at crystallization under a variety of conditions. The ^{1}H NMR spectra of these oils in CD_3CN did not reveal the presence of any paramagnetically shifted peaks, in contrast to analogous experiments performed with **2** or **3**. Several broad peaks were observed in the region 1–8 ppm which can probably be ascribed to free ligand. The ES-MS spectra of these solutions displayed a strong peak at *m/z* 231 which corresponds to $[Co(\mathbf{5})]^{2+}$, however no polynuclear complexes were detectable.

Discussion

The combination of the pyridyl-alcohol compounds **1**–**3** with CoX_2 salts and a suitable base leads to the self-assembly of a range of structurally similar dinuclear double-stranded helicates. This represents a straightforward, general and high-yielding synthetic route to transition-metal helicates.

Whilst the desired self-assembly pathway appears to be followed for **2** and **3** regardless of the nature of the base, it was noted compound **1** has a propensity to form cubane-like clusters in the presence of strong bases such as NEt_3.[16] The formation of cubane-like structures by pyridine–alcohol ligands is well documented in the literature.[17]

A wide variety of mono-anionic ancillary ligands (X) were successfully introduced into the $[Co_2(\mathbf{1})_2(\mathbf{1}\text{-H})_2X_2]$ (X = Cl, Br, I, NO_3, SCN) and $[Co_2(\mathbf{2})_2(\mathbf{2}\text{-H})_2X_2]$ (X = Cl, Br, NO_3) helicates. Within each set of helicates, there is a remarkable regularity in both the molecular structure and the packing of the helicates in the crystal structure. We also investigated the reaction of **2** with $CoSO_4$ to see whether a similar helicate may form with a di-anionic ancillary ligand. ^{1}H NMR spectroscopy indicated, however, that helicate formation was unsuccessful. Instead, this reaction produced crystals of a 1D coordination polymer, $[Co(\mathbf{1})SO_4]_8$, in which the monomeric units are linked by hydrogen bonding between the alcohol moieties and the coordinated SO_4^{2-} ions.[16] These result indicate that the overall charge neutrality of the helicates may be an important factor in their formation and/or crystallization.

A diverse array of substituents (R = H, CH_3, CH_2NO_2) may be introduced at the α-carbon atom of the pyridine–alcohol precursor without disrupting the self-assembly process or the general structure of the helicates. On the other hand, helicate formation is rather sensitive to the nature of the substituent at the 6-position of the pyridine ring. Helicates were observed to form readily from compounds with a CH_3 group at this position, however we saw no evidence for the formation of such structures starting from compounds which have a bromine (**5**) or hydrogen (**6**, **7**) in this position. The van der Waals radius of Br is similar to that of CH_3,[13] thus the failure of **5** to produce a helicate structure is unlikely to be due solely to steric effects. As the pK_{NH} of **5** is around 0.87,[18] while the pK_{NH} of **1** is 4.56,[19] these observations can probably be ascribed to the poor coordinating ability of **5**. We tentatively attribute the failure of **6** and **7** to form helicates to the existence of competing reaction pathways, and we are currently working to establish the exact nature of the actual products. It is noteworthy that potentiometric titrations have shown that, although the pK_{NH} of **6** (4.16) is lower than that of **1**, the formation of $[Cu^{II}(\mathbf{6}\text{-H})_2]$ is thermodynamically more favored than the formation of $[Cu^{II}(\mathbf{1}\text{-H})_2]$ due to destabilizing steric effects in the latter.[19]

The self-assembly of the hydrogen-bonded helicates derived from **2** and **3** is remarkably stereoselective in both solution and the solid state. One salient aspect of this diastereoselectivity is the self-association of ligand precursors of the same chirality in $[Co_2(\mathbf{3})(\mathbf{3}\text{-H})_2Cl_2]$. As the precursor compound **3** is racemic, there are two potential *homochiral* diastereomers of this helicate (in which all the units of **3** have the same absolute configuration), and four potential *heterochiral* diastereomers (in which both (*R*)-**3** and (*S*)-**3** are present). The X-ray crystal structure of $[Co_2(\mathbf{3})(\mathbf{3}\text{-H})_2Cl_2]$ reveals that a self-recognition process takes place amongst the ligand precursors to generate exclusively the two homochiral diastereomers (as a racemic mixture). Similar behavior is exhibited by $[Co_2(\mathbf{4})(\mathbf{4}\text{-H})_2Cl_2]$.[7] The ^{1}H NMR spectrum of $[Co_2(\mathbf{3})(\mathbf{3}\text{-H})_2Cl_2]$ shows that this self-sorting phenomenon also occurs in solution. It appears that the homochiral diastereoisomers of $[Co_2(\mathbf{3})(\mathbf{3}\text{-H})_2Cl_2]$ are thermodynamically more stable than their heterochiral counterparts, and this can be rationalized on steric grounds. Inspection of a molecular model clearly shows that the replacement of one units of **3** with its enantiomer will lead to an unfavorable interaction between the α-CH_3 group and a pyridyl group of the other ligand strand. The enantiomeric self-recognition of ligands in transition-metal complexes has previously been observed by ourselves[20] and others,[21] and general self-sorting phenomena in supramolecular systems have been explored in detail by Isaacs et al.[22]

A second noteworthy point concerning the diastereoselective assembly of these helicates is the interplay between the point chirality of the ligand precursors, the absolute configurations of the metal centers, and the helicity described by the ligand strands. Both metal centers in the $[Co_2(\mathbf{2})(\mathbf{2}\text{-H})_2Cl_2]$ complex adopt the *Λ* configuration in both solution and the solid state which demonstrates that the point chirality of the pyridyl-alcohol groups controls (or predetermines[5]) the absolute configuration of the metal centers. Similarly, the cobalt(II) centers in the helicates that contain (*R*)-**3** are *Λ*, whilst those associated with (*S*)-**3** adopt the *Δ* configuration. The control of the absolute configuration of the metal centers in helicates by the chirality of the ligand strands has previously been observed in conventional helicates.[1,4,5,23] The steric effects discussed above in the context of homochiral self-sorting may also be invoked to explain the observation of the present case of stereoselectivity, and indeed the phenomenon of self-sorting and chirality predetermination are closely related: The observed *Λ*,*Λ*-$[Co_2((R)\text{-}\mathbf{3})((R)\text{-}\mathbf{3}\text{-H})_2Cl_2]$ diastereomer may be converted to *Δ*,*Δ*-$[Co_2((R)\text{-}\mathbf{3})((R)\text{-}\mathbf{3}\text{-H})_2Cl_2]$ by inverting the metal centers, or it may be converted to the enantiomer of the latter helicate (*Λ*,*Λ*-$[Co_2((S)\text{-}\mathbf{3})((S)\text{-}\mathbf{3}\text{-H})_2Cl_2]$) by replacing the (*R*)-**3** units with (*S*)-**3**. The overall helicity of the dinuclear assemblies is intimately related to the absolute configurations of the metal centers,[1] thus the ligand strands of the *Δ*,*Δ* complexes describe *M* (left-handed) helices, whereas those of the *Λ*,*Λ* complexes describe *P* (right-handed) helices.

The self assembly process leading to the $[Co_2(\mathbf{2})_2(\mathbf{2}\text{-H})_2X_2]$ helicates could be conveniently monitored by ^{1}H NMR, UV/Vis and CD spectroscopies. At all Co/**2** ratios, there was no spectroscopic evidence for the formation of any complexes (other than the helicates) in significant concentration. In accord with these observations, the spectrophotometric titration of **2** with $Co(NO_3)_2$ could be fitted with just $[Co_2(\mathbf{2})_2(\mathbf{2}\text{-}$

H)$_2$] (which serves as a model for [Co$_2$(**2**)$_2$(**2**-H)$_2$(NO$_3$)$_2$] as we did not treat the anion explicitly) and free cobalt(II) as the absorbing species. Although our hypotheses concerning the exact mechanism of the self-assembly process remain speculative, we envisage that the helicates assemble by a hierarchical process[24] in which coordination of two pyridine–alcohol units to a cobalt(II) ion is followed by a deprotonation/dimerisation step to give the final assembly [Eq. (2)]. This proposal is based on the fact that metal-ligand bonding is significantly stronger than hydrogen bonding therefore the CoL$_2$ building blocks are more likely to form prior to any hydrogen-bonded species such as a putative preformed ligand strand "[L(L-H)]". Further, the alcohol moieties are rendered more acidic by coordination to the metal ion, and are well positioned for dimerization as two hydrogen bonds may form in a concerted step. Hydrophobic interactions between pyridine rings of different ligand strands, as detected by X-ray crystallography, may play a role in the final step by stabilizing the helicate structure. The fact that mononuclear complexes are not detected in significant quantities may indicate that the self-assembly process is cooperative, although the accurate assessment of relevant stepwise equilibrium constants would be required to examine this point in more detail.[25]

$$2\,\mathrm{Co} + 4\,\mathrm{L} \overset{K_1}{\rightleftharpoons} 2[\mathrm{CoL_2}] \overset{K_2}{\rightleftharpoons} [\mathrm{Co_2L_2(L{-}H)_2}] + 2\,\mathrm{H^+} \qquad (2)$$

The stability constant calculated for formation of [Co$_2$(**2**)$_2$(**2**-H)$_2$(NO$_3$)$_2$] indicates that these assemblies are only formed in appreciable amounts at relatively high concentrations. This was verified experimentally by monitoring the CD and ^{1}H NMR spectra of [Co$_2$(**2**)(**2**-H)$_2$Cl$_2$] upon dilution. These results indicate that dissociation of the helicates is significant at concentrations below about 0.01 M, and that the equilibria in Equation (2) are driven to the far left-hand side to produce free **2** (rather than any mononuclear complexes).

Conclusion

A wide range of dinuclear double-stranded helicates in which the ligand strands are built up using hydrogen bonding self-assemble upon mixing precursors **1**–**3** with CoX$_2$ salts. The straightforward synthesis of these helicates enabled us to undertake a systematic investigation of the self-assembly process. In the present report, we have focused on the variables highlighted in Figure 11.

We have found that a range of mono-anionic ancillary ligands (X) can be incorporated into these complexes. Helicate formation is also not particularly sensitive to the nature of the R group connected to the α-carbon center; precursors with R = H, CH$_3$, and CH$_2$NO$_2$ all led to similar structures. For pyridyl-alcohol compounds where this carbon is a stereogenic center, the chirality at this point can control the absolute configuration of the metal centers and the sense of helicity of overall structure. The nature of the substituent at the 6-position of the pyridyl ring is of significance, however, with precursors featuring H or Br substituents failing to produce hydrogen-bonded helicates.

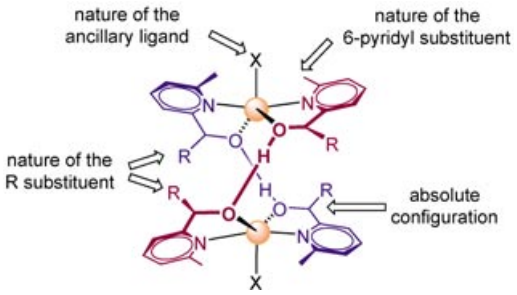

Figure 11. The variables in the self-assembly of hydrogen-bonded helicates discussed herein.

The [Co$_2$(**2**)$_2$(**2**-H)$_2$X$_2$] were found to be soluble and stable in a certain polar solvents which enabled spectroscopic characterization of the self-assembly process. These results showed that the helicates are the *only* complexes to be formed; however, their self-assembly is only efficient at relatively high concentrations. At lower concentrations, the helicates dissociate to give free **2** and cobalt(II).

The major remaining point at which diversity may be introduced into these structure—the identity of the metal ion—is the focus of current investigations in our laboratory. We are also interested in the possible applications of these helicates as building blocks for extended multidimensional arrays, and the intriguing prospect that the helicate chirality may be able to be controlled by chiral ancillary ligands.

Experimental Section

General: ^{1}H NMR spectra were recorded on a JEOL Alpha spectrometer at 500 MHz at 21 °C and referenced to the residual solvent peak (CD$_3$CN, δ = 1.95 ppm; CD$_2$Cl$_2$, δ = 5.32; CDCl$_3$, δ = 7.26 ppm). ^{13}C NMR were recorded at 125 MHz and were reference to the residual solvent peak (CDCl$_3$, δ = 77.2 ppm). UV/Vis absorbance data were recorded by using a Shimadzu UV-3150 spectrometer, and extinction coefficients are given in units of M^{-1} cm^{-1}. Solution CD spectra were recorded on a JASCO J720 spectropolarimeter at 25 °C, and $\Delta\varepsilon$ values are given in units of M^{-1} cm^{-1}. Solid state CD spectra were measured as KBr discs on the purpose-built JASCO J800-KCM spectrophotometer,[26] and were corrected for artifacts arising from linear dichroism and linear birefringence. ES-MS spectra were recorded on a Applied Biosystems Mariner spectrometer with a flow rate of 5 μL min^{-1}. Nozzle potentials and temperature (40–70 °C) were kept to a minimum to reduce fragmentation. Microanalyses were performed by Toray Research Centre, Eigiyoo, Tokyo. Unless otherwise stated, chemicals were purchased from Wako, TCI, or Aldrich and used as received. Dried solvents were used for all reactions and measurements.

Preparation of *R*-(6-methylpyridn-2-yl)ethan-1-ol (2): Compound **2** was prepared by the asymmetric hydrogenation of 2-acetyl-6-methylpyridine[27] according to the method reported by Ikariya et al.[11] for similar acetyl compounds. The compound was purified by column chromatography on SiO$_2$ using ethyl acetate/methanol (98/2) as the eluent. The *ee* was determined to be 93% by HPLC analysis using a Diacel AD-H column (150 mm × 4.6 mm, hexane/2-propanol/NEt$_3$ 98/2/0.1, 35 °C, flow rate = 1.0 mL min^{-1}). The retention times of both enantiomers were determined

using a sample of **3** ($S=7.27$ min and $R=8.03$ min).[28] ^{1}H NMR (500 MHz, $CDCl_3$): $\delta=1.53$ (m, 3H; CH_3), 2.60 (s, 3H; py-CH_3), 4.81 (br, 1H; OH), 4.93 (q, 2H; CH), 7.11–7.15 (m, 2H), 7.66 ppm (t, 1H); ^{13}C NMR (125 MHz, $CDCl_3$): $\delta=24.32$, 24.44, 68.77, 117.31, 122.33, 137.92, 157.22, 162.46 ppm; ORD: $[\alpha]_{26}^{D}=19.6$ ($c=0.30$ in $CHCl_3$); UV (CH_3CN): 265 nm (3350); CD (CH_3CN): 267 nm (−1.54).

Preparation of *rac*-(6-bromopyridn-2yl)ethan-1-ol (5): 6-Bromo-2-acetylpyridine (600 mg, 3.0 mmol) was dissolved in dry CH_3OH (8 mL) and cooled in an ice-water bath. $NaBH_4$ (340 mg, 9.0 mmol) was added in portions with stirring, and the evolution of a gas was apparent. The reaction mixture was warmed to room temperature and stirred for 2 h. The solvent was then removed and the colorless residue partitioned between CH_2Cl_2 and H_2O. The organic layer was separated, dried over $MgSO_4$ and the solvent removed to give **5** as a colorless oil. Yield: 540 mg (89%). ^{1}H NMR ($CDCl_3$): $\delta=1.50$ (d, 3H; CH_3), 3.35 (br s, 1H; OH), 4.87 (q, 1H; CH), 2.29 (d, 1H), 7.38 (d, 1H), 7.55 ppm (t, 1H); ^{13}C NMR ($CDCl_3$): $\delta=24.24$, 69.27, 118.70, 126.77, 139.39, 141.23, 165.35 ppm.

Complexes of 1

$[Co_2(\mathbf{1})_2(\mathbf{1}\text{-H})_2Cl_2]$: $CoCl_2\cdot 6H_2O$ (45.6 mg, 0.157 mmol) and **1** (77.2 mg, 0.627 mmol) were mixed in CH_3CN (1.5 mL) to give a crimson precipitate which was filtered off and washed with MeOH and diethyl ether. Yield 39.2 mg (73%). Elemental analysis calcd (%) for $[Co_2(\mathbf{1})_2(\mathbf{1}\text{-H})_2Cl_2]\cdot H_2O$ ($C_{28}H_{36}N_4O_5Co_2Cl_2$): C 48.2, H 5.2, N 8.0; found: C 48.7, H 5.4, N 7.7; IR (KBr): $\tilde{\nu}=3433$ (br m), 1607 (s), 1578 (m), 1472 (s), 1375 (m), 1171 (m), 1126 (br m), 1097 (m), 1015 (s), 949 (br s), 926 (m), 787 (m) cm^{-1}.

$[Co_2(\mathbf{1})_2(\mathbf{1}\text{-H})_2Br_2]$: $CoBr_2\cdot 6H_2O$ (46.4 mg, 0.142 mmol) was added to a solution of **1** (70.0 mg, 0.568 mmol) in CH_3CN (1.5 mL). A crimson crystalline precipitate formed rapidly. The reaction mixture was refrigerated overnight and the precipitate was isolated by filtration and washed with MeOH and Et_2O. Yield: 49.0 mg (90%). Elemental analysis calcd (%) for $C_{28}H_{34}Br_2Co_2N_4O_4$: C 43.77, H 4.46, N 7.29; found: C 44.0, H 4.6, N 6.4; IR (KBr disc): $\tilde{\nu}=3423$ (br m), 2851 (m), 1607 (s), 1578 (m), 1472 (s), 1375 (m), 1279 (w), 1244 (m), 1171 (m), 1128 (br m), 1097 (m), 1015 (m), 949 (br s), 926 (m), 858 (m), 779 (m), 733 (w) cm^{-1}.

$[Co_2(\mathbf{1})_2(\mathbf{1}\text{-H})_2I_2]$: $CoI_2\cdot 2H_2O$ (65.6 mg, 0.188 mmol) was added to a solution of **1** (92.6 mg, 0.752 mmol) in CH_3CN (1.5 mL). The deposition of a crimson-violet precipitate began almost immediately. The reaction mixture was refrigerated overnight and the precipitate isolated by filtration and washed with MeOH and Et_2O. Yield: 72.9 mg (90%). Elemental analysis calcd (%) for $C_{28}H_{34}Co_2I_2N_4O_4$: C 39.00, H 3.97, N 6.50; found: C 39.6, H 4.2, N 5.5; IR (KBr disc): $\tilde{\nu}=3423$ (br m), 2848 (m), 1605 (m), 1578 (m), 1470 (s), 1375 (m), 1242 (m), 1169 (m), 1126 (br m), 1097 (m), 1015 (m), 947 (br s), 923 (m), 854 (m), 789 (m), 731 (w) cm^{-1}.

$[Co_2(\mathbf{1})_2(\mathbf{1}\text{-H})_2(NO_3)_2]$: $Co(NO_3)_2\cdot 6H_2O$ (45.6 mg, 0.157 mmol) was added to a solution of **1** (77.2 mg, 0.627 mmol) in MeOH (400 μL). The deposition of a rose-coloured precipitate began almost immediately. The reaction mixture was refrigerated overnight and the precipitate isolated by filtration and washed with MeOH and Et_2O. Yield: 42.0 mg (73%). Elemental analysis calcd (%) for $C_{28}H_{34}Co_2N_6O_{10}$: C 45.91, H 4.68, N 11.47; found: C 46.0, H 4.8, N 11.0; IR (KBr disc): $\tilde{\nu}=3414$ (br m), 2826 (m), 1605 (m), 1578 (m), 1466 (s), 1385 (s), 1294 (s), 1163 (m), 1114 (br m), 1082 (m), 1013 (m), 957 (br m), 926 (w), 839 (w), 779 (m), 731 (w), 660 (m), 517 (m) cm^{-1}.

$[Co_2(\mathbf{1})_2(\mathbf{1}\text{-H})_2(SCN)_2]$: $Co(SCN)_2$ (44.4 mg, 0.25 mmol) and $Co(OAc)_2$ (63.1 mg, 0.25 mmol) were combined in CH_3OH (2 mL) and **1** (124.8 mg, 1.01 mmol) was added to give a crimson precipitate which was filtered off, washed with MeOH and diethyl ether, and air dried. Refrigeration of the filtrate produced violet crystals which were suitable for X-ray crystallography. Total yield: 110 mg (60%). Elemental analysis calcd for $C_{30}H_{34}Co_2N_6O_4S_2$: C 49.73, H 4.73, N 11.60; found: C 49.4, H 4.8, N 11.4; IR (KBr): $\tilde{\nu}=3423$ (br m), 2849 (m), 2073 (vs), 1607 (m), 1580 (m), 1472 (s), 1375 (w), 1171 (m), 1124 (br m), 1096 (m), 1015 (m), 953 (br m), 926 (m), 868 (m), 779 (m), 735 (w) cm^{-1}.

Complexes of 2

$[Co_2(\mathbf{2})_2(\mathbf{2}\text{-H})_2Cl_2]$: Compound **2** (188 mg, 1.37 mmol) was dissolved in MeOH (4 mL) and $CoCl_2\cdot 4H_2O$ (81.5 mg, 0.343 mmol) and $Co(OAc)_2\cdot 4H_2O$ (85.3 mg, 0.343 mmol) to give a violet solution. The solution was concentrated slowly under reduced pressure until crimson-violet crystals began to form. Et_2O was layered on top of this solution which was refrigerated for 48 h. The crystals were then filtered off, washed with a minimum amount of cold (−10°C) MeOH then Et_2O. Yield: 180 mg (71%). Elemental analysis calcd (%) for $[Co_2(\mathbf{2})_2(\mathbf{2}\text{-H})_2Cl_2]\cdot 2(CH_3OH)$ ($C_{34}H_{50}N_4O_6Co_2Cl_2$): C 51.1, H 6.3, N 7.0; found: C 50.7, H 5.8, N 6.7; ^{1}H NMR (CD_3CN, 0.01 M): $\delta=-27.65$ (3H), −8.06 (1H), 21.14 (1H), 22.79 (1H), 34.92 ppm (3H); UV/Vis (CH_3CN, 5.5×10^{-3} M): $\varepsilon=628$ nm (94.3), 525 nm (61.6), 264 nm (13200); CD (CH_3CN, 5.5×10^{-3} M): $\Delta\varepsilon=746$ nm (1.16), 532 nm (1.49), 502 (sh, 1.23), 311 nm (−1.70), 269 nm (22.3); ES-MS (CH_3CN, 0.01 M): 703.0 ($[Co_2(\mathbf{2})_2(\mathbf{2}\text{-H})_2Cl]^+$, 2%), 562.0 ($[Co_2(\mathbf{2})(\mathbf{2}\text{-H})_2Cl]^+$, 100%), 332.1 ($[Co_2\mathbf{2}_2(\mathbf{2}\text{-H})_2]^{2+}$, 12%); IR (KBr disc): $\tilde{\nu}=3420$ (br m), 2852 (m), 1605 (s), 1578 (m), 1468 (s), 1362 (s), 1312 (m), 1190 (br s), 951 (br s), 793 (m) cm^{-1}.

$[Co_2(\mathbf{2})_2(\mathbf{2}\text{-H})_2Br_2]$: Compound **2** (67.5 mg, 0.49 mmol) was dissolved in MeOH (4 mL) and $CoBr_2\cdot 4H_2O$ (40.2 mg, 0.123 mmol) and $Co(OAc)_2\cdot 4H_2O$ (30.6 mg, 0.123 mmol) were added to give a violet solution which was concentrated slowly under reduced pressure until crimson-violet crystals began to form. Et_2O was layered on top of this solution which was then refrigerated for 48 h. The crystals were then filtered off and the filtrate put aside. The crystals were washed with a minimum amount of cold (−10°C) MeOH then Et_2O, and air-dried. The first filtrate was layered with more Et_2O and refrigerated to give a second crop of product. Total yield: 59 mg (58%). Elemental analysis calcd (%) for $[Co_2(\mathbf{2})_2(\mathbf{2}\text{-H})_2Br_2]\cdot H_2O$ ($C_{32}H_{44}Br_2Co_2N_4O_5$): C 45.63, H 5.26, N 6.65; found: C 45.8, H 5.2, N 6.1; ^{1}H NMR (CD_3CN, 0.01 M): $\delta=-26.87$ (3H), −7.14 (1H), 2.20 (obscured by solvent peak), 22.20 (1H), 24.25 (1H), 33.96 ppm (3H); UV/Vis (CH_3CN, 4.6×10^{-3} M): $\varepsilon=745$ nm (sh, 29.8), 633 nm (91.0), 604 nm (92.2), 533 nm (70.2), 263 nm (16000); CD (CH_3CN, 4.6×10^{-3} M): $\Delta\varepsilon=747$ nm (1.71), 533 nm (2.16), 502 nm (sh, 1.91), 310 nm (−2.26), 271 nm (24.1), 252 nm (−2.90); ES-MS (CH_3CN, 0.01 M): 606.0 ($[Co_2(\mathbf{2})(\mathbf{2}\text{-H})_2Br]^+$, 100%); IR (KBr disc): $\tilde{\nu}=3415$ (br m), 2968 (m), 2866 (m), 1605 (s), 1578 (m), 1468 (s), 1364 (m), 1312 (w), 1244 (m), 1161 (m), 1128 (br m), 937 (br s), 872 (m), 793 (m), 752 (m) cm^{-1}.

$[Co_2(\mathbf{2})_2(\mathbf{2}\text{-H})_2(NO_3)_2]$: Compound **2** (68.7 mg, 0.50 mmol) was dissolved in CH_3CN (1 mL) and was added to a solution of $Co(NO_3)_2\cdot 4H_2O$ (35.8 mg, 0.123 mmol) and $Co(OAc)_2\cdot 4H_2O$ (30.6 mg, 0.123 mmol) in MeOH (150 μL) to give a violet solution which was concentrated slowly under reduced pressure. A rose-coloured crystalline precipitate deposited. The precipitate was suspended in a mixture of CH_3CN and Et_2O (1/3) and was isolated by filtration, washed with cold (−10°C) CH_3CN then Et_2O, and air-dried. Yield: 57.0 mg (58%). Elemental analysis calcd (%) for $[Co_2(\mathbf{2})_2(\mathbf{2}\text{-H})_2(NO_3)_2]\cdot CH_3OH$ ($C_{33}H_{46}Co_2N_6O_{11}$): C 48.30, H 5.65, N, 10.24; found: C 48.6, H 5.7, N 9.7; ^{1}H NMR (CD_3CN, 0.01 M): $\delta=-41.86$ (3H), −2.15 (1H), 1.13 (1H), 25.61 (1H), 26.11 (1H), 50.27 ppm (3H); UV/Vis (CH_3CN, 4.6×10^{-3} M): $\varepsilon=514$ nm (48.1), 265 nm (15 200). CD (CH_3CN, 4.6×10^{-3} M): $\Delta\varepsilon=615$ nm (0.58), 517 nm (0.99), 471 nm (0.71), 292 nm (−2.72), 269 nm (19.0); ES-MS (CH_3CN, 0.01 mol L^{-1}): 589.1 ($[Co_2(\mathbf{2})(\mathbf{2}\text{-H})_2NO_3]^+$, 100%); IR (KBr disc): $\tilde{\nu}=3433$ (br m), 2978 (m), 2866 (m), 1607 (m), 1466 (m), 1385 (s), 1285 (m), 1165 (m), 1084 (m), 1013 (m), 935 (w), 870(w), 806 (m), 754 (w), 681 (w) cm^{-1}.

Complexes of 3

$[Co_2(\mathbf{3})_2(\mathbf{3}\text{-H})_2Cl_2]$: This helicate was prepared as described above for **2**. X-ray quality crystals could be grown by recrystallisation from hot CH_3NO_2. ^{1}H NMR (CD_2Cl_2): $\delta=-27.94$ (3H), −8.24 (1H), 21.21 (1H), 22.91 (1H), 35.11 ppm (3H).

Spectrophotometric titrations: All operations were performed at 25°C in a controlled-temperature environment using the UV/Vis instrumentation described above. A solution of $Co(NO_3)_2\cdot 6H_2O$ (ca. 0.4 mol L^{-1}) was titrated into a solution of **2** and NEt_3 (2/1 ratio, [**2**] = ca. 0.04 mol L^{-1}) to give a final Co/**2** ratio of 1/2. Spectra were recorded following the addition of each aliquot in the wavelength region 380–860 nm. A cell with a 1 cm pathlength was used. Data were analyzed with the Specfit program,[14,29] and the titration was repeated in order to obtain three stability constants which agreed with each other within the error limits estimated by the software.

X-ray crystallography: Data were collected using a Bruker APEX system with $Mo_{K\alpha}$ radiation, and were corrected for Lorentzian, polarisation, and absorption. Structures were solved by direct methods, and refined against $|F|^2$ using anisotropic thermal displacement parameters for all non-hydrogen atoms. Hydrogen atoms were placed in calculated positions except for the alcohol protons involved in hydrogen bonding which were located on the electron density difference map (except for the structure of $[Co_2(\mathbf{3})_2(\mathbf{3}\text{-H})_2Cl_2]\cdot(CH_3NO_2)$ where these protons could not be located). CCDC-244233–CCDC-244239 contain the supplementary crystallographic data for this paper. These data can be obtained free of charge via www.ccdc.cam.ac.uk/data_request/cif, by emailing data_request@ccdc.cam.ac.uk, or by contacting The Cambridge Crystallographic Data Centre, 12 Union Road, Cambridge CB21EZ, UK; fax: (+44) 1223-336-033. The structures of $[Co_2(\mathbf{1})_2(\mathbf{1}\text{-H})_2Cl_2]\cdot H_2O$, $[Co_2(\mathbf{2})_2(\mathbf{2}\text{-H})_2Cl_2]$, $[Co_2(\mathbf{4})_2(\mathbf{4}\text{-H})_2Cl_2]$ have been published previously.[7]

Acknowledgement

We are very grateful to Mr. T. Sato for assistance with the X-ray crystallography and to Dr T. Harada for measuring the solid-state CD spectra. We also extend our warm thanks to Prof. T. Ikariya for a sample of compound **7**.

[1] C. Piguet, G. Bernardinelli, G. Hopfgartner, *Chem. Rev.* **1997**, *97*, 2005.
[2] a) M. Albrecht, *Chem. Rev.* **2001**, *101*, 3457; b) A. Williams, *Chem. Eur. J.* **1997**, *3*, 15.
[3] J. Hamacek, S. Blanc, M. Elhabiri, E. Leize, A. Van Dorsselaer, C. Piguet, A.-M. Albrecht-Gary, *J. Am. Chem. Soc.* **2003**, *125*, 1541.
[4] C. Provent, A. F. Williams in *Transition Metals in Supramolecular Chemistry* (Ed.: J. P. Sauvage), Wiley, New York, **1999**, p. 135.
[5] U. Knof, A. Von Zelewsky, *Angew. Chem.* **1999**, *111*, 312; *Angew. Chem. Int. Ed.* **1999**, *38*, 303.
[6] a) M. H. W. Lam, S. T. C. Cheung, K.-M. Fung, W.-T. Wong, *Inorg. Chem.* **1997**, *36*, 4618; b) X. Sun, D. W. Johnson, D. L. Caulder, R. E. Powers, K. N. Raymond, E. H. Wong, *Angew. Chem.* **1999**, *111*, 1386; *Angew. Chem. Int. Ed.* **1999**, *38*, 1303; c) X. Sun, D. W. Johnson, D. L. Caulder, K. N. Raymond, E. H. Wong, *J. Am. Chem. Soc.* **2001**, *123*, 2752.
[7] S. G. Telfer, T. Sato, R. Kuroda, *Angew. Chem.* **2004**, *116*, 591; *Angew. Chem. Int. Ed.* **2004**, *43*, 581.
[8] B. Breit, W. Seiche, *J. Am. Chem. Soc.* **2003**, *125*, 6608.
[9] For example, see: T. J. Burchell, D. J. Eisler, R. J. Puddephatt, *Chem. Commun.* **2004**, 944; A. M. Beatty, *Coord. Chem. Rev.* **2003**, *246*, 131; Z. Qin, M. C. Jennings, R. J. Puddephatt, *Inorg. Chem.* **2001**, *40*, 6220; D. Braga, *Chem. Commun.* **2003**, 2751; C. B. Aakeroy, A. M. Beatty, J. Desper, M. O'Shea, J. Valdes-Martinez, *Dalton Trans.* **2003**, 3956; M. Tadokoro, H. Kanno, K. Kitajima, H. Shimada-Umemoto, N. Nakanishi, K. Isobe, K. Nakasuji, *Proc. Natl. Acad. Sci. USA* **2002**, *99*, 4950; X. Xu, S. L. James, D. M. P. Mingos, A. J. P. White, D. J. Williams, *J. Chem. Soc. Dalton Trans.* **2000**, 3783.
[10] For example, see: a) T. D. Hamilton, G. S. Papaefstathiou, L. R. MacGillivray, *J. Am. Chem. Soc.* **2002**, *124*, 11606; b) Z. Qin, M. C. Jennings, R. J. Puddephatt, *Chem. Commun.* **2001**, 2676; c) T. B. Norsten, K. Chichak, N. R. Branda, *Chem. Commun.* **2001**, 1794; d) D. A. Beauchamp, S. J. Loeb, *Chem. Eur. J.* **2002**, *8*, 5084; e) C. R. Bondy, P. A. Gale, S. J. Loeb, *J. Am. Chem. Soc.* **2004**, *126*, 5030; f) S. A. Dalrymple, M. Parvez, G. K. H. Shimizu, *Chem. Commun.* **2001**, 2672; g) C. J. Kuehl, F. M. Tabellion, A. M. Arif, P. J. Stang, *Organometallics* **2001**, *20*, 1956; h) P. V. Bernhardt, E. J. Hayes, *Inorg. Chem.* **2003**, *42*, 1371; i) K. Isele, V. Broughton, C. J. Matthews, A. F. Williams, G. Bernardinelli, P. Franz, S. Decurtins, *J. Chem. Soc. Dalton Trans.* **2002**, 3899; j) S. G. Telfer, A. F. Williams, G. Bernardinelli, *Chem. Commun.* **2001**, 1498; k) A. Lavalette, F. Tuna, G. Clarkson, N. W. Alcock, M. J. Hannon, *Chem. Commun.* **2003**, 2666; l) E. Freisinger, I. B. Rother, M. S. Luth, B. Lippert, *Proc. Natl. Acad. Sci. USA* **2003**, *100*, 3748; m) R. Garcia-Zarracino, H. Hopfl, *Angew. Chem.* **2004**, *116*, 1533; *Angew. Chem. Int. Ed.* **2004**, *43*, 1507; n) D. G. Kurth, K. M. Fromm, J.-M. Lehn, *Eur. J. Inorg. Chem.* **2001**, 1523.
[11] K. Okano, K. Murata, T. Ikariya, *Tetrahedron Lett.* **2000**, *41*, 9277.
[12] In the case of $[Co_2(\mathbf{1})_2(\mathbf{1}\text{-H})_2Cl_2]$, this cavity is occupied by a water molecule. However, the cavity is empty in the other helicates.
[13] L. Pauling, *The Chemical Bond*, Cornell University Press, New York, **1967**.
[14] H. Gampp, M. Maeder, C. J. Meyer, A. D. Zuberbuehler, *Talanta* **1986**, *33*, 943.
[15] No attempt was made to distinguish between precursor **2** and its deprotonated form. Also, the nitrate ions were not explicitly treated by the chemical model, but were implicitly assumed to bind quantitatively to the cobalt(II) ions.
[16] S. G. Telfer, unpublished observations.
[17] For example, see: a) A. Escuer, M. Font-Bardia, S. B. Kumar, X. Solans, R. Vicente, *Polyhedron* **1999**, *18*, 909; b) J. Yoo, A. Yamaguchi, M. Nakano, J. Krzystek, W. E. Streib, L.-C. Brunel, H. Ishimoto, G. Christou, D. N. Hendrickson, *Inorg. Chem.* **2001**, *40*, 4604; c) C. Canada-Vilalta, E. Rumberger, E. K. Brechin, W. Wernsdorfer, K. Folting, E. R. Davidson, D. N. Hendrickson, G. Christou, *J. Chem. Soc. Dalton Trans.* **2002**, 4005.
[18] Calculated by using the Advance Chemistry Development Software Solaris (V4.67) which is part of the SciFinder 2004 software package.
[19] T. J. Lane, A. J. Kanadathil, S. M. Rosalie, *Inorg. Chem.* **1964**, *3*, 487.
[20] a) S. G. Telfer, G. Bernardinelli, A. F. Williams, *Chem. Commun.* **2001**, 1498; b) S. G. Telfer, T. Sato, R. Kuroda, J. Lefebvre, D. B. Leznoff, *Inorg. Chem.* **2004**, *43*, 421; c) S. G. Telfer, T. Sato, T. Harada, R. Kuroda, J. Lefebvre, D. B. Leznoff, *Inorg. Chem.* **2004**, *43*, 6168.
[21] For example, see: a) M. A. Masood, E. J. Enemark, T. D. P. Stack, *Angew. Chem.* **1998**, *110*, 973; *Angew. Chem. Int. Ed.* **1998**, *37*, 928; b) J. M. Rowland, M. M. Olmstead, P. K. Mascharak, *Inorg. Chem.* **2002**, *41*, 1545.
[22] A. Wu, L. Isaacs, *J. Am. Chem. Soc.* **2003**, *125*, 4831.
[23] For example, see: a) A. von Zelewsky, O. Mamula, *J. Chem. Soc. Dalton Trans.* **2000**, 219; b) W. Zarges, J. Hall, J.-M. Lehn, C. Bolm, *Helv. Chim. Acta* **1991**, *74*, 1843.
[24] J. A. A. W. Elemans, A. E. Rowan, R. J. M. Nolte, *J. Mater. Chem.* **2003**, *13*, 2661.
[25] G. Ercolani, *J. Am. Chem. Soc.* **2003**, *125*, 16097.
[26] R. Kuroda, T. Harada, Y. Shindo, *Rev. Sci. Instrum.* **2001**, *72*, 3802.
[27] Z. R. Reeves, K. L. V. Mann, J. C. Jeffery, J. A. McCleverty, M. D. Ward, F. Barigelletti, N. Armaroli, *J. Chem. Soc. Dalton Trans.* **1999**, 349.
[28] This compound was prepared by the reaction of 2-acetyl-6-methylpyridine with $NaBH_4$ in methanol.
[29] Specfit/32 for Windows: http://www.bio-logic.fr/rapid-kinetics/specfit/index.html.

Received: May 17, 2004
Published online: November 18, 2004